Macromolecules **1984**, *17*, 669–677

(3) Flory, P. J. "Principles of Polymer Chemistry"; Cornell University Press: Ithaca, NY, 1953.
(4) Wall, F. T. *J. Chem. Phys.* **1943**, *11*, 527.
(5) Treloar, L. R. C. *Trans. Faraday Soc.* **1943**, *39*, 36.
(6) Flory, P. J.; Rehner, J. *J. Chem. Phys.* **1943**, *11*, 512.
(7) Kuhn, W. *J. Polym. Sci.* **1946**, *1*, 380.
(8) Flory, P. J. *Trans. Faraday Soc.* **1961**, *57*, 829.
(9) James, H. M.; Guth, E. *J. Chem. Phys.* **1943**, *11*, 455.
(10) James, H. M.; Guth, E. *J. Chem. Phys.* **1953**, *21*, 1039.
(11) Flory, P. J. *Proc. R. Soc. London, Ser. A*, **1976**, *351*, 1666.
(12) Graessley, W. W. *Macromolecules* **1975**, *8*, 186.
(13) Flory, P. J. *J. Chem. Phys.* **1977**, *66*, 5720.
(14) Flory, P. J. *Polymer* **1979**, *20*, 1317.
(15) Bastide, J.; Duplessix, R.; Picot, C.; Candau, S. *Macromolecules*, submitted for publication.
(16) Candau, S.; Bastide, J.; Delsanti, M. *Adv. Polym. Sci.* **1982**, *44*, 27.
(17) Bastide, J.; Picot, C.; Candau, S. *J. Macromol. Sci., Phys.* **1981**, *B19*, 13.
(18) Flory, P. J. *Proc. R. Soc. London, Ser. A* **1976**, *351*, 1666.
(19) Belkebir-Mrani, A.; Herz, J.; Rempp, P., *Makromol. Chem.* **1977**, *178*, 485.
(20) Akcasu, A. Z.; Summerfield, G. C.; Jahshan, S. N.; Han, C. C.; Kim, C. Y.; Yu, H. J. *J. Polym. Sci., Polym. Phys. Ed.* **1980**, *18*, 863.
(21) Benoit, H.; Koberstein, J.; Leibler, L. *Makromol. Chem., Suppl.* **1981**, *4*, 85.
(22) Wignall, G. D.; Hendricks, R. W.; Koehler, W. C.; Lin, J. S.; Wai, M. P.; Thomas, E. L.; Stein, R. S. *Polymer* **1981**, *22*, 886.
(23) Boue, F.; Nierlich, M.; Leibler, L. *Polymer* **1982**, *23*, 29.
(24) Duplessix, R. Thesis, Universite Louis Pasteur—Strasbourg, 1975.
(25) Levy, S. Thesis, Universite Louis Pasteur—Strasbourg, 1964.
(26) Pearson, D. S. *Macromolecules* **1977**, *10*, 696.
(27) Mooney, M. *J. Appl. Phys.* **1948**, *19*, 434.
(28) Rivlin, R. S. *Philos. Trans. R. Soc. London, Ser. A* **1948**, *241*, 379.
(29) Belkebir-Mrani, A.; Herz, J.; Beinert, G.; Rempp, P. *Eur. Polym. J.* **1973**, *13*, 277.
(30) Candau, S.; Peters, A.; Herz, J. *Polymer* **1981**, *22*, 1504.

Conformational Characteristics of Poly(vinyl alcohol)[†]

Romain M. Wolf and Ulrich W. Suter*

Department of Chemical Engineering, Massachusetts Institute of Technology, Cambridge, Massachusetts 02139.

Received June 1, 1983

ABSTRACT: Conformational energies of *meso*- and *rac*-2,4-pentanediol were estimated, once without account for electrostatic interactions or hydrogen bonds and then with two different electrostatic models for the hydroxyl groups. For the dimer as well as for poly(vinyl alcohol) in aqueous solution, a simple three-state rotational isomeric state model was found. Vicinal NMR coupling constants for the dimer and the characteristic ratio for PVA were computed; they are in excellent agreement with experimental data. In aprotic solutions of the dimer intramolecular hydrogen bond formation is postulated, with an associated free energy of ca. 1 kcal/mol at room temperature.

Introduction

Poly(vinyl alcohol), PVA, is a vinyl polymer of simple structure with a wide range of applications. Commonly used PVA is atactic and usually obtained by radical polymerization of vinyl acetate with subsequent hydrolysis of the side groups.[1] Predominantly isotactic as well as syndiotactic chains can be obtained by a variety of methods.[2,3]

Attempts to characterize atactic PVA in aqueous solution have been many;[4–14] results do not mutually agree very well, however, as will be discussed later. Reliable values for the characteristic ratio of PVA in solution can nevertheless be deduced.[15,16] Heretofore, no satisfactory theory for its conformational characteristics has been presented.

2,4-Pentanediol has often been used as a model compound for PVA.[17–20] The conformational analysis of 2,4-pentanediol has been performed mainly by NMR spectroscopy, and experimental coupling constants have been determined in water as well as in apolar, aprotic solvents.[17–19] In the following, a rotational isomeric state model for PVA in water will be deduced from conformational energy calculations on 2,4-pentanediol. The incidence of intramolecular hydrogen bonds in 2,4-pentanediol and PVA will be discussed in detail.

Conformational Energies

Parameters for the Calculation. The conformational energy was calculated as the sum of intrinsic torsional energy and interaction energies between pairs of nonbonded atoms.

Table I
Parameters Used in Energy Calculations

atom or group	r_i°,[a] Å	α_i,[b] Å^3	N_i[c]
H	1.3	0.42	0.9
C	1.8	0.93	5
O	1.6	0.59	7
CH_3	2.0	1.77	7

[a] Values from ref 44, incremented by +0.1 Å. [b] See ref 29. [c] See ref 27.

The C–C bonds were assigned a 3-fold intrinsic torsional energy function with a barrier $E_{\mathrm{it,C-C}} = 2.8$ kcal/mol.[21] The barrier for the rotation of C–O bonds was derived from experimental data on methanol:[22] A 3-fold, composite rotational barrier of 1.07 kcal/mol has been reported for methanol, and subtraction of van der Waals interactions (between the hydroxyl hydrogen and the methyl hydrogens) yields a barrier of $E_{\mathrm{it,C-O}} = 0.76$ kcal/mol for the 3-fold intrinsic torsional energy function. The reliability of this value was checked by rotational energy calculations for the C–O bond in ethanol: The rotational barrier between antiperiplanar and synclinal conformations is estimated to be 1.13 kcal/mol and is in good agreement with the reported mean experimental value of 1.2 kcal/mol.[23]

Nonbonded interactions between atoms separated by more than two bonds were estimated as described before[24,25] using a spliced, three-piece pair energy function[26] based on the Lennard-Jones function $f_{ij}(d_{ij}) = (a_{ij}/d_{ij}^{12}) - (c_{ij}/d_{ij}^{6})$, d_{ij} being the distance between a pair of atoms

---

[†] Dedicated to Professor Walter H. Stockmayer on his 70th birthday.

0024-9297/84/2217-0669$01.50/0

Table II
Geometrical Parameters

bond	bond length, Å
C-C	1.53
C-O	1.43
C-H	1.10
O-H	0.95
O-X[a]	0.75_5

bond angle		angle, deg
on secondary C	C-C-C	114
	C-C-H	108.5
	H-C-H	108.5
on tertiary C	C-C-C	112.3
	C-C-H	107
	C-C-O	111
	H-C-O	108.3
on O	C-O-H	108.5
	C-O-X[a]	109.7
	H-O-X[a]	109.7

[a] X is a "pseudoatom" representing the lone-pair electron couple on the oxygen.

i and j. The parameters a_{ij} and c_{ij} were evaluated[27,28] from data for the polarizability α, the effective number of electrons N_i, and the *adjusted* van der Waals radius r_i^0 given in Table I (methyl groups in 2,4-pentanediol were treated as a single spherical group of atoms). Coulombic interactions (in kcal/mol) were calculated according to $E_{\text{coul}} = (332\delta_i\delta_j)/(d_{ij}\epsilon)$, with δ_i and δ_j being the partial charges (in elementary charge units) of two atoms i and j separated by a distance d_{ij} (in Å); ϵ is the dielectric constant of the medium and was taken as 3.5 for an apolar, aprotic environment.

The calculations did not include a specific function to evaluate "hydrogen bonds". Initially, it was assumed that Coulombic interactions would suffice to define energy contributions ascribed to hydrogen bonding. The charge distribution on the oxygen was dealt with in two different approaches. First, following an idea of Jorgensen,[30] the partial charge on oxygen was equally distributed onto two pseudoatoms, X, representing the two lone-pair electron couples, the oxygen atom itself being taken as neutral. Figure 2 displays the geometry of this special representation of a hydroxyl group. The magnitudes of the partial charges on X, C, and H are -0.237, +0.217, and +0.257 elementary charges, respectively. These values were obtained from the experimental values on magnitude and orientation of the dipole moment in 2-propanol.[31] The pseudoatoms enter only into Coulombic energy calculations; the Lennard-Jones parameters a and c were set to zero for interactions involving at least one pseudoatom. In the second approach the pseudoatoms were eliminated and their combined partial charges assigned to the oxygen atom.

Conformational Energies of the "Dimer". All interatomic interactions in 2,4-pentanediol were calculated with the geometric parameters given in Table II. Bond lengths and bond angles were kept at fixed values. These parameters were taken from literature data on the structure of the model compounds methanol,[22] ethanol,[32] and 2-propanol.[33] Figure 1 represents a molecule of 2,4-pentanediol with all torsion angles set to zero, i.e., with an all-trans conformation for the carbon-carbon backbone and the hydroxyl hydrogens of the side chains being trans with respect to the methine hydrogen. Main-chain torsion angles, ϕ_1 and ϕ_2, are measured in the right-handed or left-handed sense, depending on the stereochemical character of the diad, in accordance with usage for vinyl polymers.[34] The side-chain torsion angles, χ_1 and χ_2, are positive when the three adjoining bonds H-O, O-C, and C-H form a left-handed helical path.

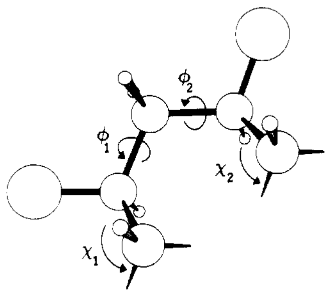

Figure 1. *meso*-2,4-Pentanediol in the conformation with all torsion angles set to zero.

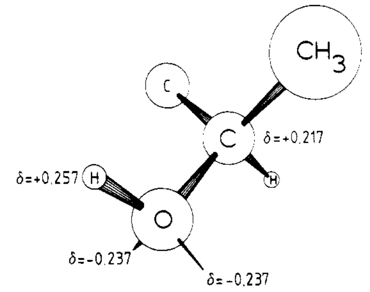

Figure 2. Fragment of 2,4-pentanediol (shown in Figure 1) indicating the placement of "pseudoatoms" (representing lone-pair electrons) and partial charges.

For the purpose of an initial assessment of the conformational characteristics of the dimers, conformational energy maps were computed.

The conformational energy was calculated as a function of ϕ_1 and ϕ_2 for every 10° in the interval from -180° to +180°. For each pair (ϕ_1,ϕ_2) side-chain rotation angles χ_1 and χ_2 were chosen that minimize the total energy. The minimization was performed with a quasi-Newton method.[35] In order to increase the probability that the global minimum with respect to χ_1 and χ_2 was reached, rather than a local one, the calculations were repeated four times with different starting values for χ_1 and χ_2, namely, (0,0), (120°,120°), (120°,0), and (-120°,0). The lowest energy of the four results was then chosen as the final value used in energy map contouring.

Plots a and b of Figure 3 show the energy contour maps for the meso and the racemic forms of 2,4-pentanediol without Coulombic interactions. Plots a and b of Figure 4 display the same maps, but including Coulombic interactions with the partial charges located on pseudoatoms according to Figure 2. Energies are given in kcal/mol relative to the respective minima in the racemic-|tt| domain.

The energy maps show that all combinations of staggered conformations are of low energy, the minima occurring almost in the exactly staggered positions. A $|g\bar{g}|$ domain under 5 kcal/mol is unusual for vinyl polymers and is due to the small radius of OH compared to common substituents in vinyl polymers.

When coulombic interactions are not included (Figure 3a,b), the maps for the racemic and the meso isomer are quite similar. The cols between |tt|, |tg|, and |gg| do not exceed 5 kcal/mol. Similarly, $|t\bar{g}|$ and $|g\bar{g}|$ are connected by a col of less than 5 kcal/mol. When Coulombic interactions are included with the partial charges on the pseudoatoms X, the conformational energies change significantly for the racemic diad. The energy with respect to |tt| increases by at least 0.5 kcal/mol for all conformations, except for $|g\bar{g}|$. For the meso diad, however, the

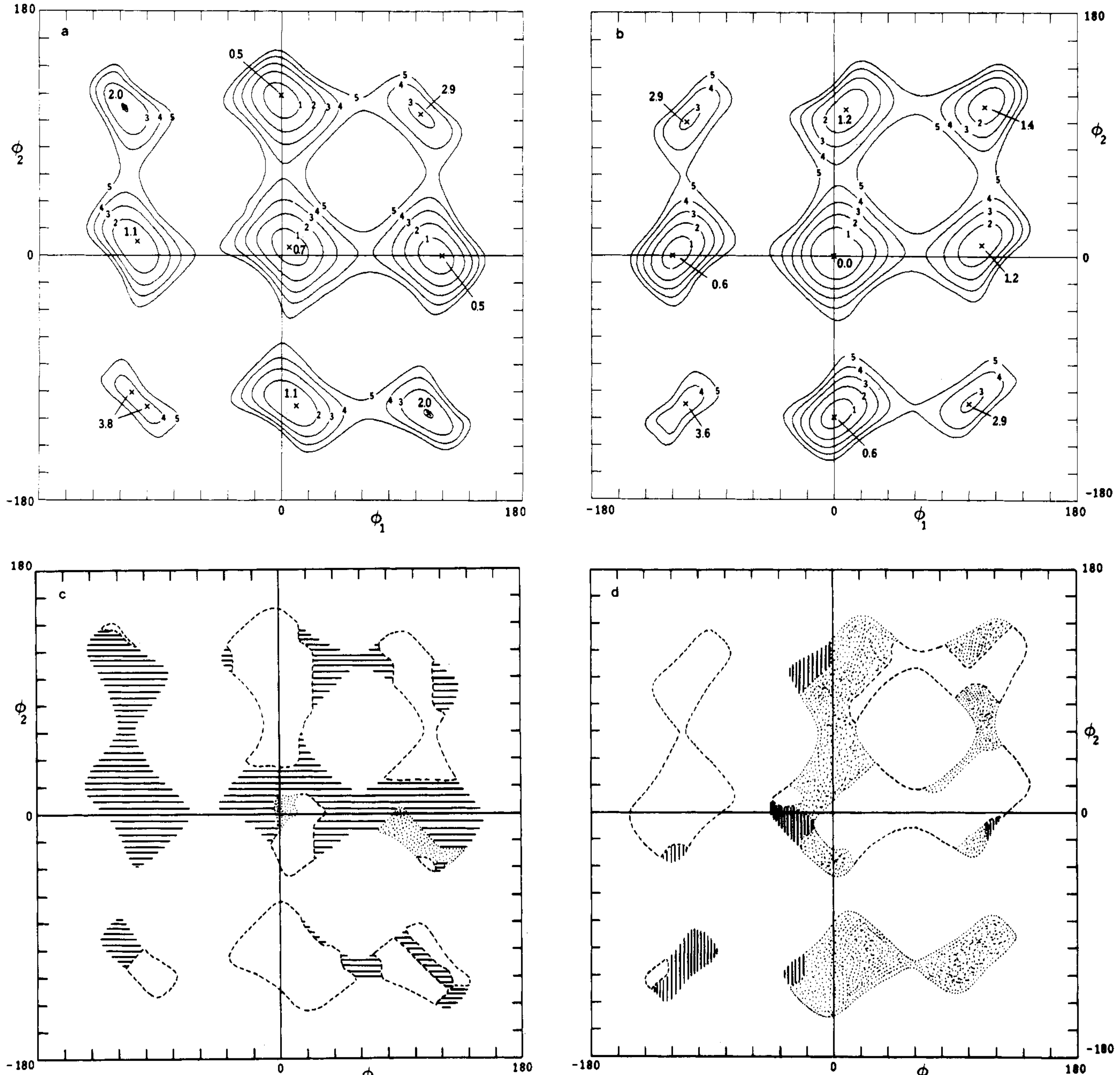

Figure 3. Energy contour maps and side-group torsion angle maps for *meso-* and *rac*-2,4-pentanediol, calculated without Coulombic interactions. Plots a and c correspond to the meso structure, and plots b and d to the racemic structure. Energy contours (in plots a and b) are in kcal/mol relative to the racemic-|tt| energy minimum. In the side-group torsion angle maps ((c) and (d)), dotted areas denote $-30° \leq \chi_1 \leq +30°$, hatched areas $+90° \leq \chi_1 \leq +150°$, and blank areas $-150° \leq \chi_1 \leq -90°$. Ranges for χ_2 are obtained for the meso diad (plot c) according to $\chi_2(\phi_1,\phi_2) = -\chi_1(\phi_2,\phi_1)$, and for the racemic diad (plot d) according to $\chi_2(\phi_1,\phi_2) = \chi_1(\phi_2,\phi_1)$.

changes in the domains of lowest energy (|tt|, |tg|, |t$\bar{\text{g}}$|, and |g$\bar{\text{g}}$|, as well as their mirror images) are insignificant. The remaining domains increase in energy similarly to the ones in the racemic diad.

The values for the side-group rotation angle χ_1 required to minimize the conformational energy for given ϕ_1 and ϕ_2 are also shown in Figures 3 and 4. These maps are placed directly underneath the corresponding contour maps. For convenience and legibility only regions with conformational energies of less than 5 kcal/mol are reproduced, and the total range of possible χ_1 values was subdivided into three intervals: [$-30° \leq \chi_1 \leq +30°$] is represented by dotted areas, [$+90° \leq \chi_1 \leq +150°$] by hatched areas, and [$-150° \leq \chi_1 \leq -90°$] by blank areas. In rare circumstances, usually outside the regions depicted in these maps, values for χ_1 were found to fall slightly outside the intervals above. The maps show the torsion angle of the first hydroxyl group, χ_1, only, but molecular symmetry indicates how the torsion angle of the second hydroxyl group, χ_2, can be obtained from the same maps: For the racemic diad $\chi_2(\phi_1,\phi_2) = \chi_1(\phi_2,\phi_1)$, and for the meso diad $\chi_2(\phi_1,\phi_2) = -\chi_1(\phi_2,\phi_1)$. The angle maps for the racemic diads (Figures 3d and 4d) should be perfectly symmetric; the apparent lack of symmetry in some regions of the maps indicates that two side-group orientations exist there for which the diad energy is equal.

Rotational Isomeric States

Assessment of Rotational States. Areas were demarcated in the energy maps such that their boundaries enclosed all points in a single trough, the conformational energy in the areas being not more than 5 kcal/mol (an exception was made for the |g$\bar{\text{g}}$| domains of the meso form, where two distinct minima were assigned to the same area;

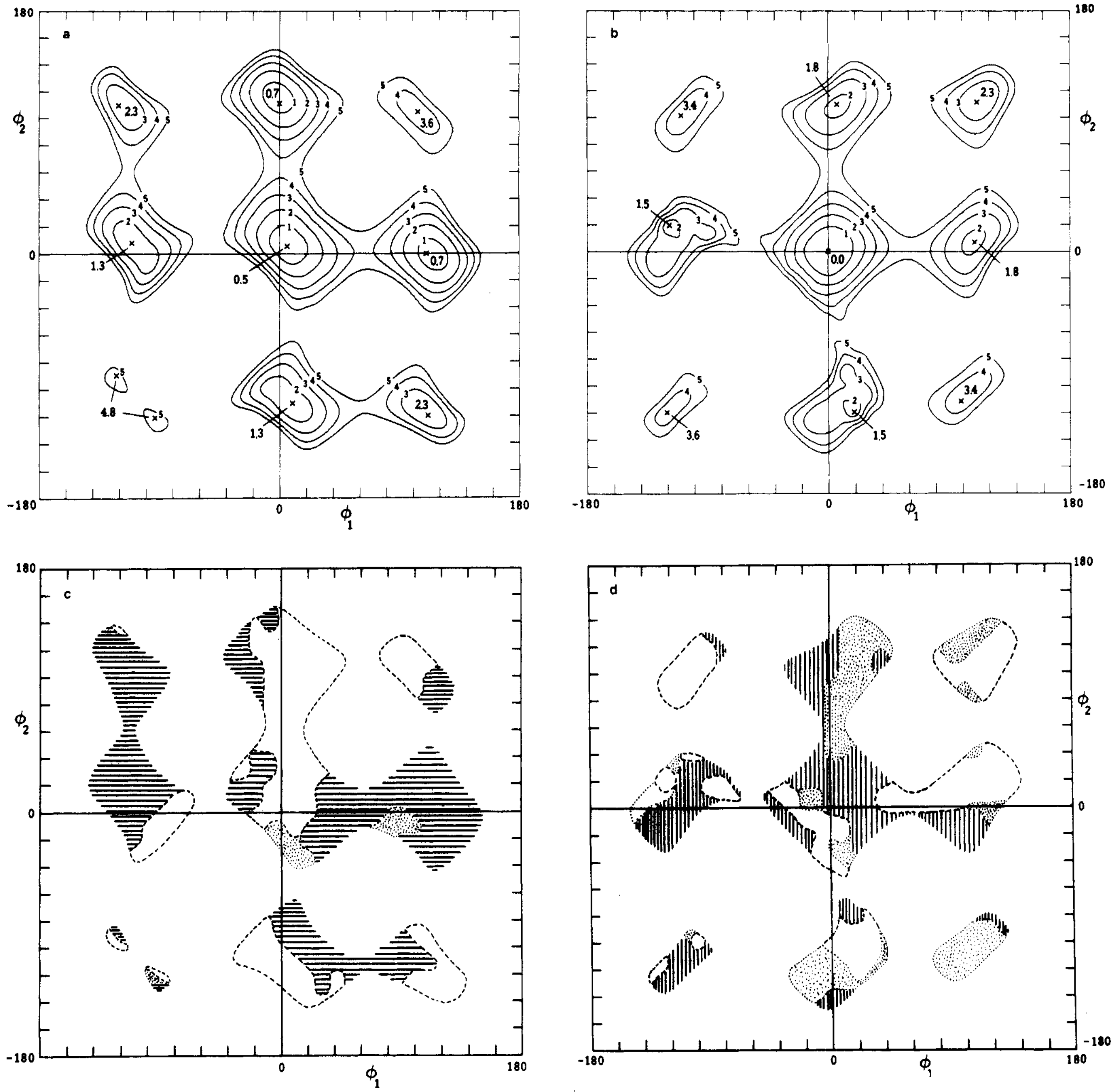

Figure 4. Energy contour maps and side-group torsion angle maps for *meso-* and *rac*-2,4-pentanediol, calculated by including Coulombic interactions with partial charges located on the pseudoatoms according to Figure 2 (Jorgensen's model). See legend to Figure 3.

this is justified by the high energy of the $|\bar{g}\bar{g}|$ domain).

The local partition function, z_ζ, the average energy $\langle E\rangle_\zeta$, and the average rotation angles, $\langle\phi_k\rangle_\zeta$ ($k = 1, 2$) for each conformational state ζ were calculated at 300 K according to

$$z_\zeta = \int_\zeta\int\int_0^{2\pi}\int_0^{2\pi}\exp(-E/RT)\ \mathrm{d}\phi_1\ \mathrm{d}\phi_2\ \mathrm{d}\chi_1\ \mathrm{d}\chi_2$$

$$\langle E\rangle_\zeta = z_\zeta^{-1}\int_\zeta\int\int_0^{2\pi}\int_0^{2\pi}E\exp(-E/RT)\ \mathrm{d}\phi_1\ \mathrm{d}\phi_2\ \mathrm{d}\chi_1\ \mathrm{d}\chi_2 \quad (1)$$

$$\langle\phi_k\rangle_\zeta = z_\zeta^{-1}\int_\zeta\int\int_0^{2\pi}\int_0^{2\pi}\phi_k\exp(-E/RT)\ \mathrm{d}\phi_1\ \mathrm{d}\phi_2\ \mathrm{d}\chi_1\ \mathrm{d}\chi_2,\quad k = 1, 2$$

Numerical integrations were performed on a 4-dimensional grid with a step size of 15°, for each of the two main-chain rotation angles and the two side-chain rotation angles, using Simpson's 1/3 rule.

The results of these integrations are given in Table III. All energies are relative to $\langle E\rangle_{\mathrm{tt,racemic}}$. The factor α is defined by

$$z_\zeta = \alpha_\zeta \exp[-\langle E\rangle_\zeta/RT] \quad (2)$$

and measures the effective size of a domain with respect to racemic-|tt|; it includes contributions from the relative torsional freedom of the side chains. In the case of the |gg| states (racemic and meso), for instance, the two hydroxyl groups can rotate freely and α is relatively high. Very low α-values are found in $|\bar{g}\bar{g}|$ states. This is due to the fact that these states have a small effective size in ϕ_1 and ϕ_2 and that both hydroxyl groups are close to each other or to a methyl group, their rotational freedom being restricted. Columns labeled "I" in Table III represent the values obtained from conformational energy calculations without Coulombic interactions. In columns labeled "II" and "III" are the results obtained from calculations including Coulombic interactions, with the partial charges

Table III
Conformational Averages for 2,4-Pentanediol at 300 K

	z			$\langle E\rangle$			α			$\langle\phi_1\rangle, \langle\phi_2\rangle$		
state	I[a]	II[a]	III[a]	I	II	III	I	II	III	I	II	III
							Meso					
tt	0.4380	0.1785	0.2115	0.43	0.84	0.96	0.9	0.7	1.1	8, 8	9, 9	8, 8
tg	0.4489	0.2967	0.3651	0.36	0.64	0.51	0.8	0.9	0.9	3, 113	2, 113	3, 113
$t\bar{g}$	0.0994	0.0909	0.0957	1.04	1.13	1.08	0.6	0.6	0.6	6, −107	7, −106	9, −108
gg	0.0160	0.0046	0.0080	2.43	3.36	2.91	0.9	1.3	1.1	103, 103	103, 103	103, 103
$g\bar{g}$	0.0338	0.0203	0.0287	1.63	2.10	1.80	0.5	0.7	0.6	111, −119	110, −118	108, −116
$\bar{g}\bar{g}$	0.0023	0.0002	0.0008	3.03	4.42	3.70	0.4	0.3	0.4	−108, −108	−109, −109	−108, −108
							Racemic					
tt	1.0000	1.0000	1.0000	0.00	0.00	0.00	1.0	1.0	1.0	3, 3	1, 1	2, 2
tg	0.1255	0.0738	0.1020	1.13	1.49	1.30	0.8	0.9	0.9	9, 107	6, 105	8, 106
$t\bar{g}$	0.2599	0.0729	0.0861	0.30	0.86	1.11	0.4	0.3	0.6	4, −116	9, −114	7, −115
gg	0.1762	0.0385	0.0676	0.84	2.01	1.57	0.7	1.1	1.0	113, 113	115, 115	115, 115
$g\bar{g}$	0.0089	0.0066	0.0095	2.51	2.80	2.47	0.6	0.7	0.6	101, −107	101, −106	102, −105
$\bar{g}\bar{g}$	0.0049	0.0021	0.0034	2.47	2.75	2.76	0.3	0.2	0.4	−116, −116	−115, −115	−110, −110

[a] I: no Coulombic interactions. II: Coulombic Interactions included; negative partial charges on the "pseudoatoms" X. III: Coulombic interactions included; negative partial charges on O.

on the pseudoatoms X (II) or on the oxygen (III). A comparison of columns II and III shows that the two schemes yield very similar results. Surprisingly, the backbone rotation angles characterizing the conformational states are nearly identical in all three cases. Rotational isomeric state angles were assigned by averaging corresponding values in Table III, weighted with the appropriate z value. We obtain $\langle\phi_t\rangle = 5°$, $\langle\phi_g\rangle = 110°$ and $\langle\phi_{\bar{g}}\rangle = -115°$, accurate to approximately 3°.

Statistical Weight Matrices and Conformational Parameters. A diad of PVA can assume the nine staggered conformations. This suggests that the general statistical weight matrices of order three[34] might be appropriate. The success of these matrices, discussed below, in reproducing the values for z_ζ and $\langle E\rangle_\zeta$ from Table III confirms this conjecture. We take

$$\mathbf{U}''_{\mathrm{m}} = \begin{bmatrix} \eta^2\omega'' & \eta & \eta\tau\omega' \\ \eta & \omega & \tau\omega' \\ \eta\tau\omega' & \tau\omega' & \tau^2\omega\omega'' \end{bmatrix}$$
$$\mathbf{U}''_{\mathrm{r}} = \begin{bmatrix} \eta^2 & \eta\omega' & \eta\tau\omega'' \\ \tau\omega' & 1 & \tau\omega \\ \eta\tau\omega'' & \tau\omega & \tau^2\omega'^2 \end{bmatrix} \qquad (3)$$

where rows and columns are indexed in the order: t, g, $\bar{g}$.[34,36] These matrices include all first-order interactions as well as intradiad second-order interactions. Inspection of models of 2,4,6-heptanetriols indicates that the statistical weight matrix describing the second-order effects in interdiad interactions, $\mathbf{U}'$, also closely resembles the traditional form:[34]

$$\mathbf{U}' = \begin{bmatrix} 1 & 1 & 1 \\ 1 & 0 & 1 \\ 1 & 1 & 0 \end{bmatrix} \qquad (4)$$

Repulsive interactions in the conformations g|g are somewhat less severe, however, than in other vinyl polymers since the size of OH is smaller than even methyl. The proper magnitude of the second-order statistical weight for g|g is slightly smaller than ω but might be significantly larger than zero.[34,37,38] Assuming that ω here is of the same order of magnitude as in polyethylene (a conjecture that is confirmed below), we anticipate a value of ca. 0.05 at 300 K. The element for g|g in $\mathbf{U}'$ should therefore be less than ca. 0.05. Experimental calculations with this element set to the actual value of ω show that its effect on the unperturbed dimensions of PVA is insignificant when compared with the results obtained with a value of zero. The matrix $\mathbf{U}'$ is therefore retained in the form given in eq 4.

Table IV
Conformational Energy Parameters from Energy Calculations[a]

E_ξ	I[b]	II[b]	III[b]	mean values used in calculations[c]
E_η	−0.39	−0.96	−0.76	
E_τ	0.00	−0.27	−0.22	
E_ω	1.83	1.81	1.56	1.73 (±0.17)
$E_{\omega'}$	0.85	0.79	0.84	0.82 (±0.04)
$E_{\omega''}$	0.32	1.01	1.04	
ξ_0	I	II	III	mean values used in calculations[c]
η_0	1.18	0.97	1.02	1.05 (±0.13)
τ_0	0.65	0.56	0.60	0.60 (±0.06)
ω_0	1.34	1.30	1.13	1.26 (±0.13)
ω_0'	1.03	0.90	1.03	0.98 (±0.09)
ω_0''	0.87	0.68	1.05	0.88 (±0.21)

[a] Energies are in kcal/mol. [b] I: no Coulombic interactions. II: Coulombic interactions included; partial charges on the "pseudoatoms" X. II: Coulombic interactions included; partial charges on O. [c] See text for explanations.

Let ξ denote one of the statistical weight parameters η, τ,... and ζ one of the states |tt|, |tg|,... for meso and racemic diads. The parameter ξ can be expressed as

$$\xi = \xi_0 \exp[-E_\xi/RT] \qquad (5)$$

Values for the E_ξ's can be evaluated by solving the overdetermined set of linear equations

$$\sum E_\xi - \langle E\rangle_\zeta = 0 \qquad (6)$$

where the $\langle E\rangle_\zeta$ values are taken from Table III. ξ_0 is found by solving the overdetermined set of linear equations

$$\sum \ln \xi_0 - \ln z_\zeta - (\sum E_\xi/RT) = 0 \qquad (7)$$

since z_ζ corresponds to the ζ-element in the $\mathbf{U}''$ matrices. The z_ζ are taken from Table III, and the values for E_ξ are the solutions of the set of eq 6. The final results for E_ξ and ξ_0 are listed in Table IV. Columns I, II, and III have the same meanings as in Table III.

Parameters describing interactions that do not involve proximity of charged atoms should be very similar in all three cases (I, II, and III), regardless of whether Coulombic interactions are included in the energy calculations or not. This is verified by the values in Table IV. E_ω and $E_{\omega'}$ are second-order energy parameters describing the interactions of two methyl groups and a methyl group with a hydroxyl group, respectively. Their values are indeed very similar for the cases I, II, and III. E_η, E_τ, and especially $E_{\omega''}$, however, are sensitive to Coulombic interactions. E_η and E_τ describe first-order interactions that reflect mainly the attraction of a positively charged C atom to a negatively charged O (or X) atom if Coulombic forces are taken into account. This attractive effect is quite large as witnessed by the decrease of both E_η and E_τ when Coulombic interactions are involved. Interactions between two hydroxyl groups in the diad are precipitated in $E_{\omega''}$. Here, the inclusion of Coulombic interactions has a striking effect. If the assumption were true that Coulombic interactions are sufficient to describe the attractive effect of hydrogen bonding, one would expect $E_{\omega''}$ to decrease in the sequence I, (II or III). However, the opposite occurs. The overall effect is not attractive, but repulsive. This fact will be considered later.

The preexponential factors ξ_0 show little sensitivity to the presence or absence of Coulombic interactions, indicating that the shape of the energy hypersurfaces is not significantly locally perturbed by the inclusion of Coulombic energy terms.

The last column in Table IV shows the mean values for those parameters that were similar for cases I, II, and III. dE_ξ and $d\xi_0$ are twice the standard deviations of the mean values. For the three energy terms E_η, E_τ, and $E_{\omega''}$, a value of dE_ξ of ±0.05 kcal/mol was selected. The dE_ξ and $d\xi_0$ values are used later to estimate the error limits of all values calculated with E_ξ and ξ_0.

Vicinal Coupling Constants of the "Dimers" and Hydrogen Bonding

Accurate experimental data on vicinal proton magnetic resonance coupling constants of the 2,4-pentanediols in water, as well as in apolar solvents, were published by Fujiwara et al.[17,18] and Doskočilova et al.[19] The results of both groups are virtually identical.

The most reliable quantities deduced from these data are the sum and the difference of the coupling constants of protons that are syn and anti in a Fischer projection[39]

$$\sum J = \langle J_{\mathrm{syn}} \rangle + \langle J_{\mathrm{anti}} \rangle$$
$$\Delta J = \langle J_{\mathrm{syn}} \rangle - \langle J_{\mathrm{anti}} \rangle \qquad (8)$$

These quantities were estimated subject to the assumption that the vicinal coupling constants, J, depend only on the dihedral angle between the pair of protons in question. Numerical values for J in individual conformations can be obtained by using the Karplus function.[40] The averages required in eq 8 can then be computed by averaging all conformational isomers:

$$\langle J_{\mathrm{k}} \rangle = \sum p_\zeta J_{\mathrm{k},\zeta} \qquad (9)$$

where k is syn or anti and p_ζ is the a priori probability of the appropriate bond (1 or 2) to be in conformation ζ; ζ stands for |tt|, |tg|,... etc. The a priori probabilities were calculated with the statistical weight parameters obtained above and shown in Tabled IV. The torsion angles, on which the $J_{\mathrm{k},\zeta}$ depend, are taken from the last columns of Table III. This procedure takes into account that ϕ_{t} in |tt| is different from ϕ_{t} in |tg|... etc. and gives slightly better agreement with experimental data than use of the average rotational isomeric state angles deduced before.

The particular attractive interaction between two hydroxyl groups, or between a hydroxyl group and water, is customarily described by "hydrogen bonding". This "bond" is strongly angle dependent and is somewhat stronger than the usual van der Waals interactions. Sometimes a special potential function in addition to electrostatic effects is used to describe it,[41] but other authors claim that the proper treatment of Coulombic interactions suffices.[30,42] Irrespective of this difference in opinion it is clear that in water or similar protic solvents a large number of intermolecular hydrogen bonds exist. The number of hydrogen bonds available to each hydroxyl group in the dimer (or in PVA) in aqueous solution is therefore probably independent of conformation. In addition, Coulombic interactions in excess of those supposedly responsible for hydrogen bonding are attenuated by the high value of the dielectric constant, ϵ. For aqueous solutions, therefore, it is appropriate to include only van der Waals energies in the nonbonded interactions.

Table V
Coupling Constants (Hz) of 2,4-Pentanediol in H_2O

	$\langle J_{\mathrm{syn}} \rangle$	$\langle J_{\mathrm{anti}} \rangle$	$\Delta J = \langle J_{\mathrm{syn}} \rangle - \langle J_{\mathrm{anti}} \rangle$	$\Sigma J = \langle J_{\mathrm{syn}} \rangle + \langle J_{\mathrm{anti}} \rangle$
		Meso		
calcd[a]	$8.8_5 \pm 0.3$	$6.9_4 \pm 0.5$	$1.9_1 \pm 0.6$	$15.7_9 \pm 0.5$
exptl[b]	7.5	5.7	1.8	13.2
		Racemic		
calcd[a]	$8.2_4 \pm 0.3$	$4.2_1 \pm 0.3$	$4.0_3 \pm 0.6$	$12.4_5 \pm 0.2$
exptl[b]	8.5	4.3	4.2	12.8

[a] See text for explanations. The parameters used in the calculations were taken from the energy computations without any adjustment. [b] Experimental data from ref 18 and 19; precision of the values is probably ±0.2 Hz.

Statistical weight matrices for aqueous solutions were obtained with E_η, E_τ, and $E_{\omega''}$ from the column labeled "I" in Table IV, i.e., −0.39, 0, and 0.32 kcal/mol, respectively, and with the remaining parameters from the last column of Table IV (i.e., $E_\omega = 1.73$, $E_{\omega'} = 0.82$, $\eta_0 = 1.05$, $\tau_0 = 0.6$, $\omega_0 = 1.26$, $\omega_0' = 0.98$, $\omega_0'' = 0.88$). A priori probabilities, p_ζ, required in eq 9, were computed, and $\langle J_{\mathrm{syn}} \rangle$, $\langle J_{\mathrm{anti}} \rangle$, $\sum J$, and ΔJ were evaluated. Comparison between ("a priori") calculated and experimental value,[18,19] shown in Table V, is excellent. We conclude that in water intramolecular hydrogen bonds do not significantly influence the conformational equilibria of the dimer.

In aprotic solvents, in contrast to the situation in water, the incidence of intramolecular hydrogen bonds can significantly favor some conformations over others. Vicinal coupling constants in the dimer have been determined in apolar solvents.[18,19] On the basis of these experimental data the authors have claimed that in the meso form the |tt| conformation is strongly favored over all other conformations by an intramolecular hydrogen bond between the two adjacent hydroxyl groups. Theoretical consideration of the conformational characteristics of the dimer are, of course, dependent on the way in which hydrogen bonds are evaluated. We chose to follow Jorgensen[30] and to assume in a first step that proper treatment of Coulombic interactions (Figure 2) might suffice to describe the tendency for hydrogen bonds. This corresponds to case II in the conformational energy calculations reported above; the maps in Figure 4 and the column labeled "II" in Table IV represent this approach. Average vicinal coupling constants computed on this basis are in agreement with experiment except for $\langle J_{\mathrm{anti}} \rangle_{\mathrm{meso}}$, which is overestimated by 5 Hz. This discrepancy far exceeds possible experimental error or uncertainty of calculations.

In order to appraise the influence of the particular features of Jorgensen's model we repeated all calculations

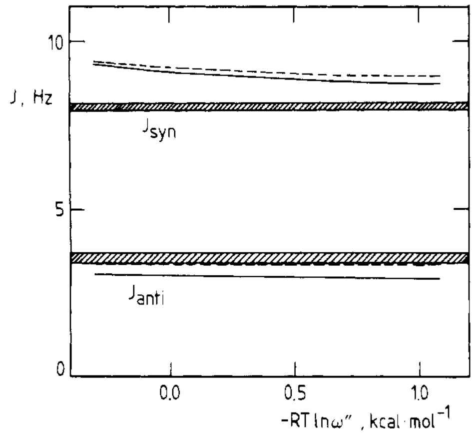

Figure 5. Vicinal coupling constants in *rac*-2,4-pentanediol in aprotic solvents as a function of the free energy of OH/OH interactions. Hatched bands represent experimental data from ref 18 and 19. Dashed lines are computed with Jorgensen's structural model and solid lines with the simpler structural model; see text.

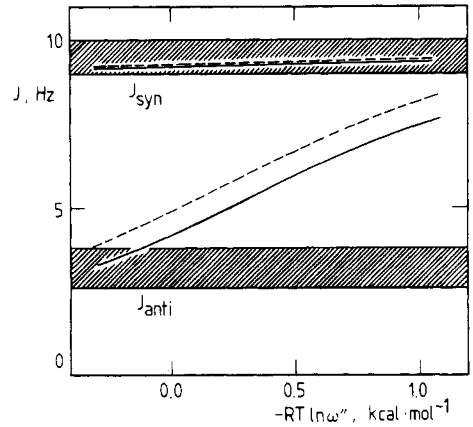

Figure 6. Vicinal coupling constants in *meso*-2,4-pentanediol in aprotic solvents as a function of the free energy of OH/OH interactions. Hatched bands represent experimental data from ref 18 and 19. Dashed lines are computed with Jorgensen's structural model and solid lines with the simpler structural model; see text.

with the structurally simpler model where the pseudoatoms, X, are eliminated and their pairwise combined partial charge is assigned to the oxygen atoms. Results of these calculations are summarized in the columns labeled "III" in Tables III and IV. Average vicinal coupling constants computed with these values did not differ significantly from those obtained with the more elaborate model (columns labeled "II"), and $\langle J_{anti} \rangle_{meso}$ differed from the experimental value by almost 5 Hz.

In an effort to identify the source of this discrepancy in aprotic solvents a posteriori, intramolecular hydrogen bonds were introduced as free energy contributions to ω'', since the effects of hydrogen bonds would most severely be felt by this parameter. Figures 5 and 6 display the effect of the free energy contribution from hydrogen bonds on the calculated vicinal coupling constants of the racemic and meso dimer, respectively. The experimental values[18,19] are represented by hatched bands, where the values in pyridine, chloroform, and methylene chloride are included. The dashed lines represent results obtained with Jorgensen's structural model, where E_η and E_τ are taken from the column labeled "II" in Table IV. Solid lines reproduce the results from the simpler structural model, where E_η and E_τ are taken from the column labeled "III" in Table IV. The predictions made with the values for $E_{\omega''}$ from Table IV lie at the right-most limit of the figures ($-RT \ln \omega''$ = ca. 1.1 kcal/mol).

The effects of a change in ω'' on the coupling constants in the racemic dimer are marginal, and the agreement between calculated and experimental values is always satisfactory. $\langle J_{syn} \rangle$ for the meso dimer likewise is almost independent of ω'' and in close agreement with the experimental value, but $\langle J_{anti} \rangle$ is strongly affected by ω''. A free energy change associated with a hydrogen bond of $\Delta(RT \ln \omega'')$ = ca. −1 kcal/mol suffices to bring calculated and experimental values into agreement. The value of ca. −1 kcal/mol thus assigned to the free energy associated with a hydrogen bond agrees in order of magnitude with other experimental evidence.[43]

Unperturbed Dimensions of PVA

Investigations of aqueous solutions of atactic PVA have been many; the results of viscosimetry[4–14] in combination with molecular weight averages obtained by light scattering,[6,8] ultracentrifugation,[6,11] and vapor pressure osmometry[4,5] allowed estimations of the unperturbed dimensions. Experimental data from different sources differ substantially, however. Possible sources of this lack of agreement are the differences in the structure of the polymer samples investigated, i.e., the degree of hydrolysis, tacticity, branching,[8] molecular weight distribution,[12] and problems due to aggregation, even at high dilution (ref 1 and 12 and references therein), possibly compounded by the fact that experimental work in water seems to be unusually difficult.

Water is not a Θ-solvent for PVA. The reported value for the exponent in the Mark–Houwink–Sakurada equation is in the range 0.6–0.75[5–12,14] (a value of 0.5 has also been reported,[13] but it is based on only three data points and it might be due to substantial experimental error). Extrapolation of viscosity measurements to Θ-conditions (by Kurata–Stockmayer plots or Burchard–Stockmayer–Fixman plots) yields values of the constant factor in the Mark–Houwink–Sakurada equation at a Θ-state, K_Θ, in the wide range 0.16–0.30 mL/g,[16] but most values lie between 0.19 and 0.24 mL/g for temperatures of about 300 K. Kurata and Stockmayer[15] recommend a value of 0.222 (±0.025) mL/g. Wolfram and Nagy[10] have tried to establish Θ-conditions for PVA in water/alcohol mixtures. Their values for K_Θ differ quite strongly from one solvent mixture to another, ranging from 0.155 mL/g in water/*tert*-butyl alcohol to 0.283 mL/g in water/ethanol. The second virial coefficients estimated from their Kurata–Stockmayer plots are not zero, however, although much smaller than in solutions in pure water. Evaluation of the combined literature on experimental data leads us, in agreement with Kurata and Stockmayer, to consider K_Θ = 0.22 (±0.03) mL/g to be a suitable value. Taking the "universal" viscosity constant $\phi = 2.6 \times 10^{23}$, we obtain a value of the characteristic ratio of PVA in water of $C_\infty = 8.5 \pm 1$.

The success of the prediction of vicinal coupling constants in aqueous solution of the 2,4-pentanediols prompted use of the ("a priori") rotational isomeric state scheme developed by calculations on the "dimer" without taking Coulombic interactions into account.

For the theoretical calculation of the characteristic ratio, common matrix generation techniques were used.[45] The polymer chain was modeled as a Bernoullian sequence of meso and racemic diads, w_m being the weight of a meso diad. The characteristic ratio $C_n = \langle r_0^2 \rangle / nl^2$ was calculated for different w_m as the average over 10 Monte Carlo trials each for $n = 200$. (The results for $n = 200$ for the isotactic and syndiotactic chains are only slightly lower than C_∞, obtained by linear extrapolation of C_n vs. $1/n$.) The parameters employed are listed in Table VI on the left.

Table VI
Parameters Used for the Characteristic Ratio

	ξ at 300 K	$\pm d\xi^a$	$\left(\frac{\partial \ln C_\infty}{\partial \ln \xi}\right)_{w_m=0.5}$
η	2.02	0.3	0.51
τ	0.60	0.08	−0.12
ω	0.07	0.02	−0.01
ω'	0.25	0.03	0.03
ω''	0.50	0.13	−0.09
	θ, deg	$\pm d\theta$, deg	$\left(\frac{\partial \ln C_\infty}{\partial \ln \theta}\right)_{w_m=0.5}$
$\pi - \theta''$	112	1	2.3
$\pi - \theta'$	114	1	1.9
	$\langle\phi\rangle$, deg	$d\langle\phi\rangle$, deg	$\left(\frac{\partial \ln C_\infty}{\partial \ln \langle\phi\rangle}\right)_{w_m=0.5}$
$\langle\phi_t\rangle$	5	3	−0.1
$\langle\phi_g\rangle$	110	3	−1.0
$\langle\phi_{\bar{g}}\rangle$	115	3	0.5

[a] See text for explanations.

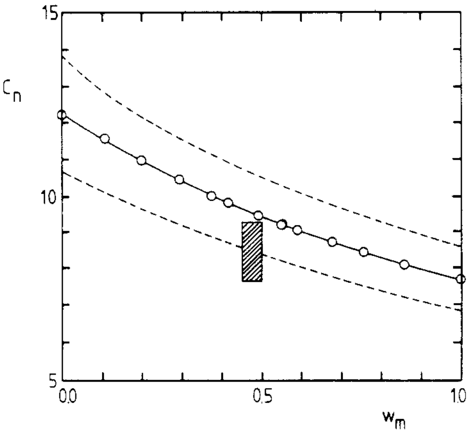

Figure 7. Characteristic ratios, $C_n = \langle r^2 \rangle_0 / nl^2$, for chains with Bernoullian tacticity and a probability for a meso diad w_m. The solid line, circles, and dashed lines represent the theoretical prediction, and the hatched rectangle displays the region indicated by experimental data; see text.

These are the values obtained directly from conformational energy calculations. To obtain confidence limits for the prediction each of these parameters was assigned an uncertainty, also shown in Table VI. The uncertainties for the statistical weights are calculated from the deviations, dE_ξ and $d\xi_0$, obtained earlier (see Table IV). Uncertainties for bond and torsion angles are intuitive estimates. Partial derivatives of C_n with respect to individual parameters are listed in the last column of Table VI for $w_m = 0.5$. The values for C_n thus calculated are $C_n = 12.2$ (±1.6) for a purely syndiotactic chain, 9.5 (±1.0) for an atactic chain with $w_m = 0.5$, and 7.8 (±0.9) for a purely isotactic chain.

Figure 7 displays the results of computations of the characteristic ratio. The circles and the solid line represent the values obtained with the parameters from Table VI. The dashed lines indicate the limits of confidence obtained by summing the variances of C_n with respect to each parameter, where the required partial derivatives are estimated numerically. The hatched rectangle in Figure 7 represents the range of experimental values for C_∞, based on the K_Θ value given by Kurata and Stockmayer,[15] together with an estimate for the frequency of meso diads in atactic PVA of 0.45–0.48[46–48] from proton and ^{13}C magnetic resonance investigations. These limits for the tacticity are typical for atactic PVA but might be somewhat too restrictive in view of the fact that the actual tacticity of the samples used to determine K_Θ had not been measured. Comparison between experiment and prediction is good. Experimental data on the chain dimensions of stereoregular PVA have not been published to our knowledge.

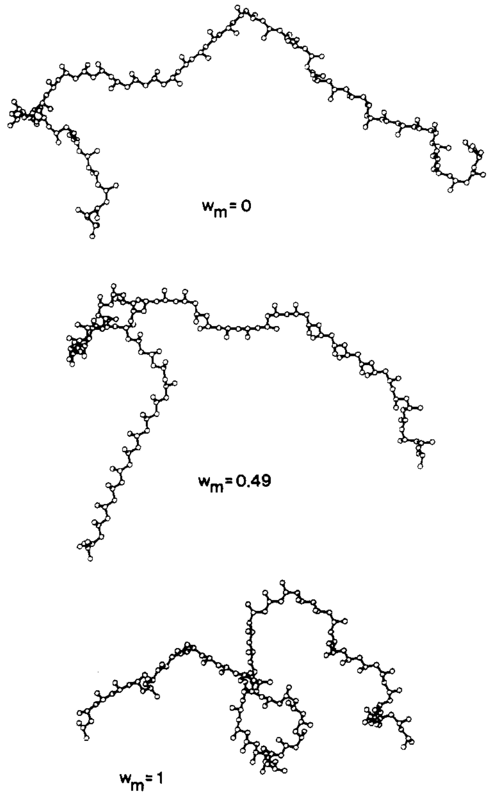

Figure 8. Simulated chains of 100 bonds for different Bernoullian tacticities; w_m is the probability for a meso diad. See text.

Conclusions

For the dimer as well as for PVA a simple three-state rotational isomeric scheme is appropriate. Bond angles are $\pi - \theta' = 114°$ and $\pi - \theta'' = 112°$; torsion angles are $\phi_t = 5°$, $\phi_g = 110°$, and $\phi_{\bar{g}} = -115°$. The statistical weights are given by

$$\begin{aligned} \eta &= 1.1 \exp(+200/T) \\ \tau &= 0.6 \\ \omega &= 1.3 \exp(-850/T) \\ \omega' &= 1.0 \exp(-400/T) \\ \omega'' &= 0.9 \exp(-150/T) \end{aligned} \tag{10}$$

The similarity between this value of E_ω (1.7 kcal/mol) and the ones found for polypropylene, polystyrene, poly(methyl acrylate), poly(vinyl acetate), and polyethylene, i.e., 1.6–2.0 kcal/mol, is gratifying. Contrary to experience with most other vinyl polymers where $\omega > \omega' > \omega''$, due to the larger size of the substituent with respect to CH_2 (or CH_3), we find here the sequence $\omega < \omega' < \omega''$, caused by the unusually small radius of OH. The introduction of explicit intramolecular hydrogen bonds into the calculations is not necessary to explain the conformational characteristics of PVA in water. In aprotic solvents, however, the dimer might form intramolecular hydrogen bonds with an associated free energy of ca. 1 kcal/mol.

A simulation of conformations of PVA chains of $x = 50$ for three different tacticities is shown in Figure 8. The chains are oriented so that the principal axes of their radius of gyration tensors are parallel. The conformational sequences were generated by recourse to an "equivalent first-order Markov scheme",[49] where a priori and conditional probabilities were computed for the chain with the particular stereostructure desired. The displayed chains were selected for close agreement of the squared end-to-end distance with the characteristic ratio for the same tacticity. Extended conformational sequences occur frequently in the atactic chain; these extended sequences, although sterically impure, could be packed into crystallites. The observed partial crystallinity of atactic PVA (ref 1 and 7 and references therein) could thus be explained.

Acknowledgment. Partial support for this work came from the Texaco–Mangelsdorf Associate Professorship. R.M.W. thanks the Schweizerischer Nationalfonds zur Foerderung der Wissenschaftlichen Forschung for a Fellowship. We thank Doros N. Theodorou for some calculations.

Registry No. *meso*-2,4-Pentanediol, 3950-21-8; *rac*-2,4-pentanediol, 1825-14-5; poly(vinyl alcohol) (homopolymer), 9002-89-5.

References and Notes

(1) Pritchard, J. G. "Poly(vinyl alcohol), Basic Properties and Uses"; MacDonald Technical and Scientific: London, 1970.
(2) Finch, C. A. In "Poly(vinyl alcohol), Properties and Applications"; Finch, C. A., Ed.; Wiley: London, 1973; Chapter 10.
(3) Murahashi, S. *Pure Appl. Chem.* **1967**, *15*, 435–52.
(4) Staudinger, H.; Warth, H. *J. Prakt. Chem.* **1940**, *155*, 276; cited in ref 5.
(5) Flory, P. J.; Leutner, S. F. *J. Polym. Sci.* **1948**, *3*, 880–90.
(6) Dieu, H. A. *J. Polym. Sci.* **1954**, *12*, 417–38.
(7) Beresniewicz, A. *J. Polym. Sci.* **1959**, *35*, 497–505.
(8) Beresniewicz, A. *J. Polym. Sci.* **1959**, *39*, 63–79.
(9) Matsumoto, M.; Ohyanagi, J. *Kobunshi Kagaku* **1960**, *17*, 191–6.
(10) Wolfram, E.; Nagy, M. *Kolloid Z.-Z. Polym.* **1968**, *227*, 86–92.
(11) Garvey, M. J.; Tadros, Th. F.; Vincent, B. *J. Colloid Interface Sci.* **1974**, *49*, 57–68.
(12) Koopal, L. K. *Colloid Polym. Sci.* **1981**, *259*, 490–8.
(13) Dialer, K.; Vogler, K.; Patat, F. *Helv. Chim. Acta* **1952**, *35*, 869–85.
(14) Lankfeld, J. M. G.; Lyklema, J. *J. Colloid Interface Sci.* **1972**, *41*, 454–65.
(15) Kurata, M.; Stockmayer, W. H. *Fortschr. Hochpolym.-Forsch.* **1963**, *3*, 196–312.
(16) Van Krewelen, D. W. "Properties of Polymers, Their Estimation and Correlation with Chemical Structure"; Elsevier: Amsterdam, 1976; p 182.
(17) Fujiwara, S.; Fujiwara, Y.; Fujii, K.; Fukuroi, T. *J. Mol. Spectrosc.* **1966**, *19*, 294–304.
(18) Fukuroi, T.; Fujiwara, Y.; Fujiwara, S.; Fujii, K. *Anal. Chem.* **1968**, *40*, 879–89.
(19) Doskočilova, D.; Štokr, J.; Votavová, E.; Schneider, B.; Lim, D. *J. Polym. Sci., Part C* **1967**, *16*, 2225–37.
(20) Shimanouchi, T. *Pure Appl. Chem.* **1966**, *12*, 287–309.
(21) Abe, A.; Jernigan, R. L.; Flory, P. J. *J. Am. Chem. Soc.* **1966**, *88*, 631–9.
(22) Lees, R. M.; Baker, J. G. *J. Chem. Phys.* **1968**, *48*, 5299–318.
(23) Kakar, R. K.; Seipt, P. J. *J. Chem. Phys.* **1972**, *57*, 4060–1.
(24) Suter, U. W. *J. Am. Chem. Soc.* **1979**, *101*, 6481–96.
(25) Suter, U. W.; Saiz, E.; Flory, P. J. *Macromolecules* **1983**, *16*, 1317–28.
(26) The Lennard-Jones pair function, $f(d)$, is truncated at d^*, a cubic polynomial is spliced between $f(d)$ at $d_l = d^* - h/2$ and the constant level $f(d^*)$ at $d_r = d^* + h/2$, and the resulting function is shifted by $f(d^*)$ to yield $E_{vdW} = 0$ for $d \geq d_r$. The function is

$$E_{vdW}(d) = f(d) - f(d^*) \qquad \text{for } d < d_l$$

$$\begin{aligned} E_{vdW}(d) = \left(\frac{\partial f(d)}{\partial d}\right)_{d_l}(d_r - d)^2(d - d_l)/h^2 + \\ f(d_l)(d_r - d)^2[2(d - d_l) + h]/h^3 + \\ f(d^*)(d - d_l)^2[2(d_r - d) + h]/h^3 - f(d^*) \qquad \text{for } d_l \leq d < d_r \end{aligned}$$

$$E_{vdW}(d) = 0 \qquad \text{for } d_r \leq d$$

In this paper d^* was 4.5 Å, and h was 1 Å.
(27) Pitzer, K. *Adv. Chem. Phys.* **1959**, *2*, 59–83.
(28) Brant, D. A.; Miller, W. G.; Flory, P. J. *J. Mol. Biol.* **1967**, *23*, 47–65.
(29) Ketelaar, J. "Chemical Constitution"; American Elsevier: New York, 1958.
(30) Jorgensen, W. L. *J. Am. Chem. Soc.* **1980**, *102*, 543–9.
(31) Kondo, S.; Hirota, E. *J. Mol. Spectrosc.* **1970**, *34*, 97–107.
(32) Culot, J. P. 4th Austin Symposium on Gas Phase Molecular Structure, 1972, Paper T8.
(33) Aziz, N.; Rogowski, F. *Z. Naturforsch., B* **1966**, *21b*, 966.
(34) Flory, P. J.; Sundararajan, P. R.; DeBolt, L. G. *J. Am. Chem. Soc.* **1974**, *96*, 5015–24.
(35) Fletcher, R. AERE Report No. R-7125, 1972, Harwell, England; Subroutine VA10A in Harwell Subroutine Library, 1972, Harwell, England.
(36) η is the first-order parameter expressing the statistical weight of the trans relative to the gauche state, τ represents the statistical weight of the gauche-bar relative to the gauche state, and second-order interactions are characterized by ω, ω', and ω'' for interactions between CH_n/CH_n, CH_n/OH, and OH/OH, respectively, n being 2 or 3; i.e., methyl and methylene groups are regarded as equal for these interactions.
(37) Abe, A. *J. Polym. Sci., Polym. Symp.* **1976**, *No. 54*, 135–44.
(38) Abe, A. *Macromolecules* **1977**, *10*, 35–43.
(39) Two protons are syn when they lie on opposite sides of the all-trans backbone and anti when they lie on the same side.
(40) Bovey, F. A. "High Resolution NMR of Macromolecules"; Academic Press: New York, 1972; p 36.
(41) McGuire, R. F.; Momany, F. A.; Scheraga, H. A. *J. Phys. Chem.* **1972**, *76*, 375–93.
(42) Brink, G.; Glasser, L. *J. Comp. Chem.* **1982**, *3*, 219–26.
(43) Pimental, G. C.; McClellan, A. L. "The Hydrogen Bond"; W. H. Freeman: San Francisco, 1960; Chapter 10.
(44) Bondi, A. *J. Phys. Chem.* **1964**, *68*, 441–51.
(45) Flory, P. J. *Macromolecules* **1974**, *7*, 381–92.
(46) Moritani, T.; Kurama, I.; Shibatani, K.; Fujiwara, Y. *Macromolecules* **1972**, *5*, 577–80.
(47) Wu, T. K.; Ovenall, D. W. *Macromolecules* **1973**, *6*, 582–4.
(48) Wu, T. K.; Sheer, M. L. *Macromolecules* **1977**, *10*, 529–31.
(49) Flory, P. J. "Statistical Mechanics of Chain Molecules"; Interscience: New York, 1969; Chapter III.8.